Direct Femtosecond Laser Inscription of High-Order Bragg Gratings in Fluoroaluminate Glass Fiber

Lin She, Niannian Xu, Pengfei Wang, Jiquan Zhang, Mo Liu, Nian Lv, Ruoning Wang, Zhenrui Li, Shijie Jia, Shunbin Wang, Gerald Farrell, and Weimin Sun

***Abstract*—This letter reports the fabrication of fiber Bragg gratings (FBGs) within in-house fabricated fluoroaluminate (AlF_3) glass fibers using femtosecond (fs) laser inscription at 800 nm. The grating strength of the FBGs was investigated for different pulse energies and different orders, and a 3rd-order FBG with Bragg wavelength at 1557 nm was found to have the highest reflectivity of 99.5%. In addition, the reflectivity of the mid-IR grating peaks for different orders was also studied, and a 2nd-order FBG with a reflectivity of 98.8% was obtained at 2864 nm. Finally, the temperature characteristics of a mid-IR FBG were studied between 30 °C and 150 °C, showing a linear wavelength dependence and an excellent stability for the refractive index modulation. Such highly reflectivity FBGs in AlF_3 fiber have significant potential for applications in the development of compact all-fiber mid-IR fiber lasers.**

***Index Terms*—Fiber Bragg gratings, fluoroaluminate glass fiber, femtosecond laser.**

I. Introduction

FLUORIDE glass with a low phonon energy and broad spectral transmission window ranging from Ultraviolet (UV) to Mid-Infrared (MIR) have been widely investigated for fiber amplifiers and fiber lasers, especially for MIR fiber lasers since the 1980s. The applications of MIR lasers include medical surgery, communication, sensing, material processing, molecular spectroscopy and pump sources for other lasers [1]–[6]. Typical fluoride glasses, such as fluorozirconate (ZrF_4), fluoroindate (InF_3) and fluoroaluminate (AlF_3) glasses have been well developed as a range of excellent host materials for long wavelength (λ) lasing emission. The cavity reflectors in MIR laser structures can use either dichroic mirrors (DMs) which involves a free-space coupling method or use FBGs which allows for an all-fiberized structure.

FBGs have attracted a significant level of attention in recent decades given their high reflectivity, good wavelength selectivity and narrow reflection linewidth. As is well known, an all-fiber laser structure using an FBG as a cavity reflector can achieve a higher efficiency and a much more compact size compared with lasers using dichroic mirrors. Furthermore, the use of DMs can significantly increase the complexity and potential for instability of the laser system. For fiber laser applications, FBGs are commonly written either directly in the doped active fiber, or in a section of undoped fiber which is then spliced to the laser's active fiber. A number of FBG fabrication methods have been developed, such as UV exposure and direct laser writing techniques.

To date, the fabrication of FBGs in fluoride fibers has focused mainly on ZrF_4 and InF_3 glass-based fibers. For example, in 2007, Bernier *et al.* reported an FBG written using a femtosecond (fs) laser with a refractive index modulation of $\Delta n \sim 10^{-3}$ in Tm^{3+} -doped ZBLAN fibers [7], and also showed that the formation of gratings was related to the negative refractive index change induced by the femtosecond laser. In 2018, Aydin *et al.* inscribed a 99.5% high reflectivity FBG and an 8% low reflectivity FBG in Er^{3+} -doped ZBLAN fiber and demonstrated a laser output power of 41.6 W at 2.8 μm [8]; this is the highest laser output reported at $\sim$3 μm in which FBGs played an important role in increasing the output power. In the work reported in [8] the FBGs were written using a phase mask technique. Phase masks can only write gratings with a specific period or with only small variations possible in the period, whereas the fs laser direct-writing technique allows for the flexible selection of the grating period Λ, the Bragg wavelength (λ_B), the grating order and its physical length and thus the reflectivity [9]. In 2017, Bharathan *et al.* wrote FBGs with a reflectivity of $\sim$50% in a Ho^{3+}/Pr^{3+} co-doped double-cladding ZBLAN fiber using line-by-line direct-writing technique, and achieved a laser output

Manuscript received February 10, 2022; revised March 9, 2022; accepted March 11, 2022. Date of publication March 16, 2022; date of current version March 30, 2022. This work was supported in part by the National Natural Science Foundation of China under Grants 61935006, 62090062, 62005060, 61905048, and 62005061, in part by the National Key R&D Program of China under Grant 2020YFA0607602, in part by the Joint Research Fund in Astronomy under cooperative agreement between the National Natural Science Foundation of China and Chinese Academy of Sciences under Grant U2031132, in part by the Shenzhen Basic Research Project under Grant JCYJ20190808173619062, in part by the 111 project to the Harbin Engineering University under Grant B13015, and in part by the Heilongjiang Touyan Innovation Team Program. *(Lin She and Niannian Xu are co-first authors.) (Corresponding author: Pengfei Wang.)*

Lin She, Niannian Xu, Jiquan Zhang, Mo Liu, Nian Lv, Ruoning Wang, Zhenrui Li, Shijie Jia, Shunbin Wang, and Weimin Sun are with the Key Laboratory of In-Fiber Integrated Optics of Ministry of Education, College of Science, Harbin Engineering University, Harbin 150001, China (e-mail: lshe@hrbeu.edu.cn; xuniannian@hrbeu.edu.cn; 1037706223@qq.com; liumo@hrbeu.edu.cn; lvnian56@163.com; ruonwang@hrbeu.edu.cn; lizr20@hrbeu.edu.cn; jiasj@hrbeu.edu.cn; shunbinwang@hrbeu.edu.cn; sunweimin@hrbeu.edu.cn).

Pengfei Wang is with the Key Laboratory of In-Fiber Integrated Optics of Ministry of Education, College of Science, Harbin Engineering University, Harbin 150001, China, and also with the Key Laboratory of Optoelectronic Devices and Systems of Ministry of Education and Guangdong Province, College of Optoelectronic Engineering, Shenzhen University, Shenzhen 518060, China (e-mail: pfwang@szu.edu.cn).

Gerald Farrell is with the Photonics Research Center, Technological University Dublin, Grangegorman Campus, D07 EWV4 Dublin, Ireland (e-mail: gerald.farrell@tudublin.ie).

Digital Object Identifier 10.1109/JPHOT.2022.3159556

efficiency of 17% at $\lambda \sim 2.88$ μm [10]. In 2018, Goya *et al.* fabricated an FBG with 97% reflectivity and $\Delta n \sim 1.1\times10^{-3}$ in Er^{3+} -doped ZBLAN fiber using a plane-by-plane direct-writing technique, demonstrating a laser output efficiency of 29.1% at $\lambda \sim 2.8$ μm [11]. In 2019, Bharathan *et al.* wrote an FBG with a maximum grating coupling coefficient of $\kappa \sim 464$ m^{-1} using the so-called stacking direct-writing method [12]. FBGs were also inscribed in fluoroindinate (InF_3) fibers; in 2020, Bharathan *et al.* wrote a grating with a high reflectivity at $\lambda \sim 4$ μm and $\kappa \sim 275$ m^{-1} after annealing at a temperature of $T \sim 150$ °C for 90 minutes [13].

Compared with ZrF_4 and InF_3 glass, AlF_3 has shown a good chemical and mechanical stability. AlF_3 glass has a higher glass transition temperature (~370 °C) and much better resistance (typically in the order of ten times better) to water corrosion than typical ZrF_4, ZBLAN and InF_3 glasses [14], [15]. Therefore, AlF_3 fiber has a great potential to develop a practical high-power MIR fiber laser at room temperature without the complexity of additional environmental protection, for example, Wang *et al.* obtained a 10.4% laser output efficiency at $\lambda \sim 2.9$ μm by pumping a Ho^{3+}/Pr^{3+} co-doped AlF_3 fiber in 2019 [16]. Liu *et al.* obtained a room-temperature laser at $\lambda \sim 2.9$ μm with a maximum 1.13 W output power in a Ho^{3+}/Pr^{3+} co-doped AlF_3 fiber in 2021 [17]. In both of these two examples, the fiber lasers utilised DMs, but it is very likely that performance of these AlF_3 fiber lasers could be further improved if the DMs are replaced by FBGs in the laser cavity, to develop higher power MIR fiber lasers.

Fs laser is a powerful tool for manufacturing various microstructures inside transparent materials due of its very short pulse width and extremely high peak power. FBGs fabricated by a direct fs laser inscription in fluoride glass fibers offers extreme flexibility in terms of structure design compared with phase mask method. This paper reports FBGs operating at $\lambda_B \sim 1557$ nm and $\lambda_B \sim 2864$ nm, which are successfully inscribed into AlF_3 fibers using an fs laser and a line-by-line direct-writing method. The temperature dependence of the inscribed AlF_3 FBGs are also investigated.

II. Fabrication of FBGs in ALF_3 Fiber

The AlF_3 fiber used in the experiment was custom-fabricated by using the rod-in-tube method. The glass composition was $30AlF_3$-$10BaF_2$-$19CaF_2$-$9.5YF_3$-$12.5SrF_2$-$2.5PbF_2$-$3.5MgF_2$-$3LiF$-$10ZrF_4$ (in mol.%) for the core and $30AlF_3$-$10BaF_2$-$20CaF_2$-$10.5YF_3$-$13SrF_2$-$3.5MgF_2$-$3LiF$-$10ZrF_4$ (in mol%) for the cladding.

Fig. 1 shows a schematic setup of the fs laser direct-writing system used in this work to fabricate FBGs. A Ti: Sapphire femtosecond laser system (Solstice Ace) emits pulses at $\lambda \sim 800$ nm with a repetition rate of 1 kHz and a duration of 100 fs (full width half-maximum, FWHM). A beam splitter with ratio of 9:1 was placed after the fs laser to reduce the fs laser energy reaching the target fiber to 10%. Fig. 2(a) shows the microscope image of the cross section of the customized AlF_3 fiber, which has a core diameter of 10.5 μm, a NA ~0.27, a cladding diameter of 225 μm, providing few-modes guidance at $\lambda \sim 1550$ and ~2864 nm.

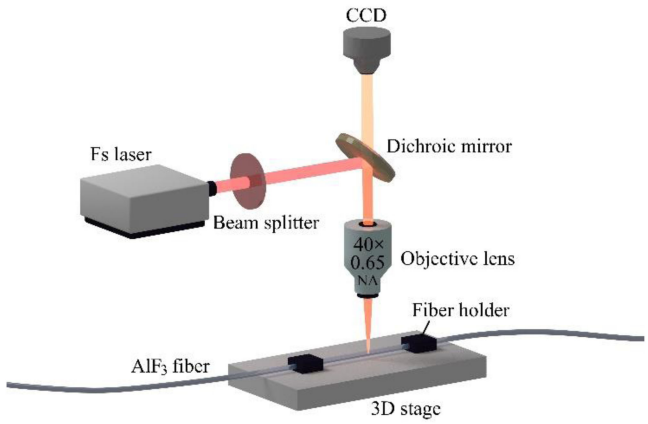

Fig. 1. Schematic of fs laser fabricating FBGs system.

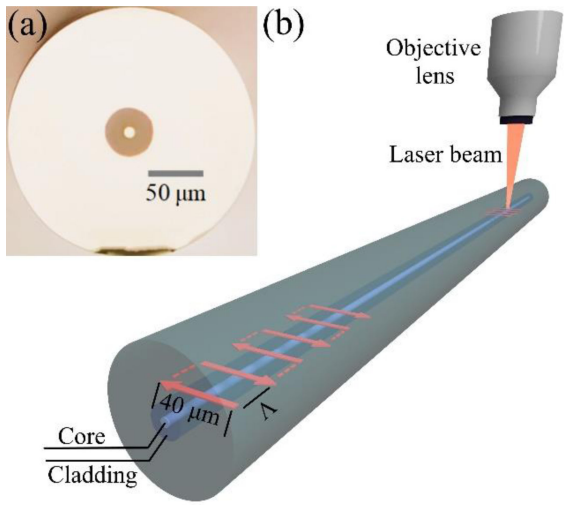

Fig. 2. (a) Microscopic image of the transverse cross section of AlF_3 fiber. (b) The path of the writing pattern for uniform FBG inscription (top-view).

The background loss at $\lambda \sim 793$ nm for the fiber was measured as circa 1.9 dB/m. For FBG inscription, the laser beam was focused into the core of the AlF_3 fiber using a 40× objective (Olympus) with a numerical aperture (NA) of ~0.65. To avoid aberrations at the curved air-glass interface, the section of AlF_3 fiber over which inscription took place was immersed in refractive index matching oil and then covered with a glass coverslip with a thickness of 100 μm. The fiber was held straight by a three-dimensional motorized translation stage (Newport X: XMS100-S; Y: XMS100-S; Z: VP-5ZA, XPS-D). Each grating plane was directly inscribed by moving the fiber in relation to the focus point of the laser beam over a distance of 40 μm. As shown in Fig. 2(b), each of the 40 μm wide grating planes is separated by a distance Λ. A mechanical shutter was used to block the laser pulse train during the movements represented by the dashed path.

According to coupled mode theory, λ_B, is defined as $2n_{eff}\Lambda/m$, where n_{eff} is the effective refractive index of the core area, and m is the grating order. The reflectivity R of a grating with length

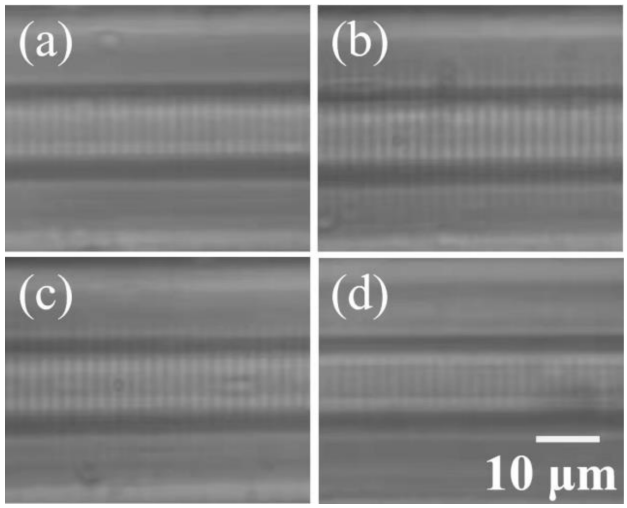

Fig. 3. Microscope images of FBGs inscribed with E_p of (a) 2.25 μJ (top view), (b) 4.5 μJ (top view) and (c, d) 3.6 μJ, (c: top view; d: side view).

L can be expressed as:

$$R = \tanh^2(\kappa L) \tag{1}$$

While κ depends on Δn and λ_B according to: [18]

$$\kappa = \pi \Delta n / \lambda_B \tag{2}$$

In order to estimate the optimal pulse energy (E_p) to use, a series of fourth order gratings with $L = 9$ mm, $\Lambda \sim 2.07$ μm and $\lambda_B \sim 1557$ nm were written for six different E_p values of ~ 2.25 μJ, 2.7 μJ, 3.15 μJ, 3.6 μJ, 4.05 μJ and 4.5 μJ, respectively. The inscription speed for all the FBGs was 80 μm/s. The total inscription time of each FBG was approximately 1 h. Fig. 3(a) and (b) show the microscope images of the FBGs inscribed with $E_p \sim 2.25$ μJ and 4.5 μJ. The grating plane inscribed with $E_p \sim 2.25$ μJ exhibits a very small Δn, while that at $E_p \sim 4.5$ μJ is significantly larger. A supercontinuum source (YSL, SC Series) was butt-coupled into the AlF_3 fiber, and an optical spectrum analyzer (OSA, Yokogawa AQ6370D) with a 500-pm resolution was used to assess the transmission spectra after the FBGs were inscribed.

Fig. 3(a) and (b) shows the microscope images of the FBGs inscribed with an E_p of (a) 2.25 μJ and (b) 4.5 μJ for the top of view, and Fig. 3(c), (d) shows the top and side microscope views respectively of the resulting grating when the pulse energy is 3.6 μJ. From the side view, it is obvious that the grating has been written through the entire core, which leads to a large mode overlap factor.

Fig. 4 shows the FBG transmission spectra for $E_p \sim 2.25$ μJ, 2.7 μJ, 3.15 μJ, 3.6 μJ, 4.05 μJ and 4.5 μJ. The corresponding resonance dips were 2.7 dB ($R = 46.3\%$), 5.4 dB ($R = 71.2\%$), 7.6 dB ($R = 82.6\%$), 17 dB ($R = 98\%$), 9.9 dB ($R = 89.8\%$) and 7.5 dB ($R = 82.2\%$). The split peaks at $E_p \sim 3.15$ μJ, 3.6 μJ, 4.05 μJ and 4.5 μJ were attributed to the defocusing of the lens due to the flow of index-matching oil during writing induced by heating of the oil at higher E_p values. As the grating planes deviated from perpendicularity to the core longitudinal direction along the laser focus point direction, in a few-mode fiber they induce cross-coupling, because of asymmetry [19]. The short-wavelength side of the Bragg peak has a side peak for $E_p \sim 3.15$ μJ, 3.6 μJ, while it is minimal for $E_p \sim 4.05$ μJ, possibly because of more symmetrical structure of the test fiber.

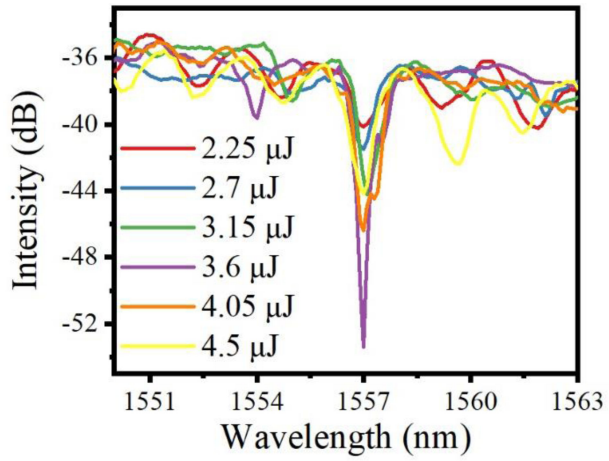

Fig. 4. Transmission intensity spectra of the FBGs at pulse energies from 2.25 μJ, to 4.05 μJ.

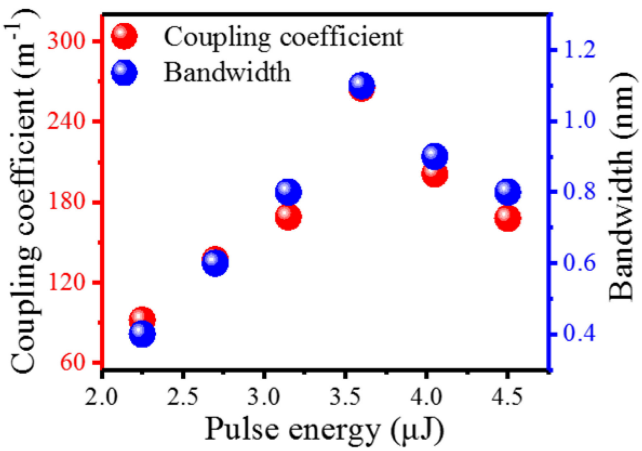

Fig. 5. The FBG coupling coefficient and 3-dB bandwidth as a function of the fs laser pulse energy.

III. Optical Characterization of ALF_3 FBGs

From the FBG transmission spectra shown in Fig. 4, the reflectivities R and thus the coupling coefficients, were obtained as 92 m^{-1}, 137 m^{-1}, 169 m^{-1}, 265 m^{-1}, 201 m^{-1} and 168 m^{-1}, respectively, for the six values above, shown in Fig. 5 as a function of E_p. From Fig. 5, one can see that the coupling coefficient κ initially rises, reaches a maximum value at 265 m^{-1} and then falls to 168 m^{-1}. The increase can be attributed to an increase in Δn caused by the gradual increase of pulse energy, while the fall could be a result of damage in the core, possibly due to the energy exceeding the damage threshold of the AlF_3 fiber. The κ reached its maximum at $E_p \sim 3.6$ μJ. In addition, given the importance of the 3-dB bandwidth in many FBG applications, Fig. 5 also shows the variation of the 3 dB bandwidth as a function of E_p. The change in the 3 dB bandwidth follows

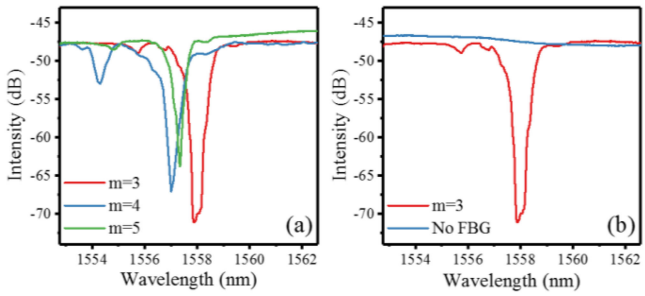

Fig. 6. (a) Transmission spectra of the 3rd, 4th and 5th-order FBGs. (b). Comparison of transmitted intensity between in fiber with a 3rd-order FBG inscribed and a bare fiber with no FBG.

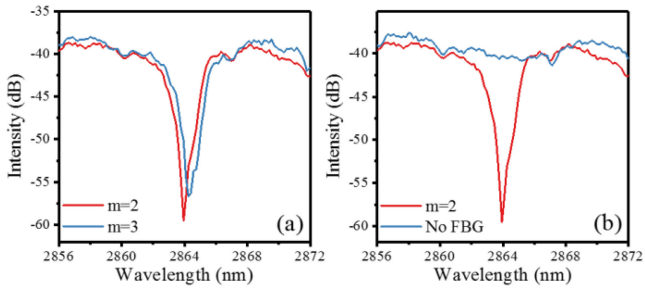

Fig. 7. (a) Transmitted intensity spectra of the 2nd and 3rd-order FBGs. (b). Transmission intensity of fibers with 2nd-order FBGs and no FBGs.

the change in the coupling coefficient, with a maximum 3 dB bandwidth of 1.1 nm circa an E_{p} ~3.6 μJ.

As an E_{p} value ~3.6 μJ was found to offer the highest coupling coefficient and thus grating strength this value of pulse energy was used to investigate the effect of grating order m on FBGs inscribed in an AlF_3 fiber. With E_{p} set to ~3.6 μJ, several FBGs at λ_B ~1557 nm but with different orders were written nm in the AlF_3 fiber. The grating length was $L = 10$ mm for all the FBGs and the grating period Λ was ~1.553 μm, 2.07 μm and 2.587 μm, for m = 3, 4, and 5, respectively. Fig. 6(a) shows that the biggest resonance dip of 23.2 dB ($R = 99.5\%$) occurs for m = 3. The resonance dip for m = 4 and 5 was 18.5 dB ($R = 98.6\%$) and 16.5 dB ($R = 97.8\%$). With an increasing m, the resonance strength of the FBG gradually decreases. This can be easily explained by the decreasing number of grating planes present for a fixed *L*. The FWHM bandwidths of the 3rd, 4th and 5th-order FBGs were measured as 1.24 nm, 0.95 nm and 0.42 nm respectively. The FBG out-of-band loss was also estimated, Fig. 6(b) which shows the transmission spectra of two fibers with a 3rd-order FBG and no FBG structure: for the FBG case, the short-wavelength side is lower corresponding to a loss of ~1.1 dB/cm.

Different order FBGs were also written near λ_B ~2864 nm at E_{p} ~3.6 μJ. A mid-IR supercontinuum source was assembled and an OSA (Yokogawa AQ6377) with a 500-pm resolution was used for the spectral characterization. The length = 10 mm for all FBGs while the grating period Λ was ~1.92 μm and 2.88 μm for m = 2 and m = 3, respectively. Fig. 7(a) shows that the dip of the 2nd-order FBG was 19.2 dB ($R = 98.8\%$), larger than that of the 3rd-order of 16.9 dB ($R = 98\%$). The measured FWHM

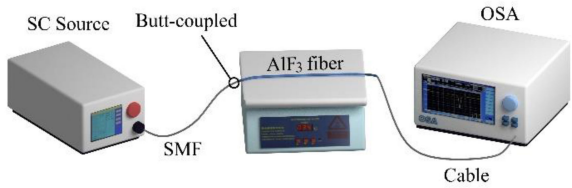

Fig. 8. Schematic diagram for FBGs heat treatment test.

bandwidths are estimated as 2.56 nm and 2.29 nm for m = 2 and m = 3, respectively. The insertion loss of the 2nd-order FBG was estimated at the short-wavelength side to be ~1.1 dB/cm.

The insertion losses of the two fabricated FBGs are still relatively large but a number of further improvements can be undertaken to reduce such loss [12], [20]. For example, the optimization of laser writing conditions can be further refined by changing the focusing objectives to ones with a different NA and in addition consideration could be given to using a direct writing process that is performed multiple times but with a lower pulse energy each time. Finally, improvements can be made to the fabrication process for the fiber, such as ensuring a more uniform refractive index distribution and better core-cladding concentricity, which in turn can significantly improve the quality of the inscribed FBGs and thus reduce the insertion loss.

IV. Temperature Characteristics and Heat Treatment of the ALF_3 FBGs

The temperature characteristics of the FBGs was investigated by recording the mid-IR spectra circa 2865 nm of a 2nd-order FBG at different temperatures. Fig. 8 shows the experiment setup used to study the temperature stability. Thermal grease was used to help maintain the temperature of the AlF_3 fiber and the oven consistent throughout the process.

The temperature was first increased from 30 °C to 150 °C in steps of 20 °C, and was maintained constant for 20 min at each temperature, as shown in Fig. 9(a). After 60 mins at 150 °C, with recording every 20 mins, see Fig. 9(b), the grating temperature was decreased to 30 °C (see Fig. 9(c)). All the corresponding spectra were recorded with a 200-pm resolution. As the temperature increased, the resonance dip first increased to 13.9 dB (70 °C) and then decreased to 10.2 dB (150 °C) from the initial 12.4 dB (30 °C) (see Fig. 9(d)). A 2.84 nm red shift in the grating wavelength was observed during this process, which differs from the blue shift observed in ZBLAN and InF_3 fibers [11], [12]. It is also found that the 3-dB bandwidth decreases from 1.56 nm at 30 °C to 1 nm at 150 °C. At a fixed temperature *T* ~150 °C, the dip reduced by 0.3 dB, and remained constant at 9.9 dB after 40 min. Then, as the temperature decreased, it was found that the resonance dips were not restored to their original values at the corresponding temperature, which demonstrates that the refractive index change induced by thermal annealing in the AlF_3 fiber is permanent and irreversible. Furthermore, the center wavelength of the FBG has an excellent linear relationship with the temperature. The inset in Fig. 9(d) presents a significant red shift when *T* increased, and a significant blue shift when *T* decreased. During the FBG heat treatment, both λ_B and Δn are

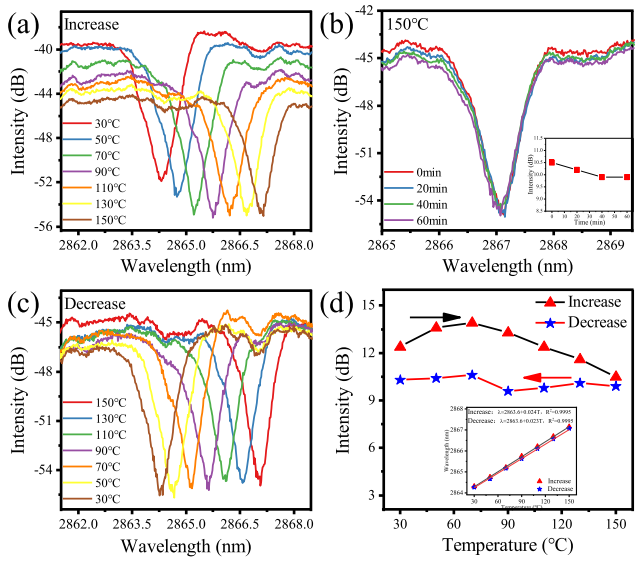

Fig. 9. (a) Transmission spectra of the FBG when T increased from 30 °C to 150 °C; (b) Transmission spectra of the FBG when T was maintained at 150 °C for 60 min (inset: Bragg wavelength peak strength *vs.* time); (c) Transmission spectra of the FBG when T decreased from 150 °C to 30 °C; (d) Bragg wavelength peak strength when T was changed from 30 °C to 150 °C (inset: experimental data and linear fit between central wavelength and temperature).

affected by the material thermal expansion and the thermo-optic effect [21].

The two FBGs show good potential to be used in high power lasers in the mid-infrared region. As a measure of their suitability for use in a fiber laser, the fabricated FBGs provide high reflectivity, good wavelength selectivity and a narrow reflection linewidth. The FBGs therefore have the potential to be used to replace DMs as cavity reflectors and are thus a significant step toward in realizing all-fiber mid-infrared laser systems. The use of such FBGs in turn will allow for less physical complexity and further improvements in power scaling and the stability of mid-infrared fiber lasers.

V. Conclusion

In conclusion, this is the first report of 1557 nm and 2864 nm FBGs written in AlF_3 fibers. The optimal pulse energy was investigated and a value of 3.6 μJ was found to provide FBGs with the highest grating strength. A 3rd-order FBG with a reflectivity of 99.5% and low insertion loss ($<$1.1 dB/cm) was obtained by using a line-by-line method at 1557 nm. A 2nd-order FBG with a 98.8% reflectivity and $<$1.1 dB/cm insertion loss was also obtained by using the same method at 2864 nm. A heat treatment process from 30 °C to 150 °C resulted in a 2.84 nm red shift of the central wavelength and a minimal permanent change of the refractive index modulation. This research paves the way for more extensive FBG applications for all-fiber mid-IR lasers.

References

[1] A. S. Kurkov *et al.*, "Mid-IR supercontinuum generation in Ho-doped fiber amplifier," *Laser Phys. Lett.*, vol. 8, no. 10, pp. 754–757, 2011.

[2] S. D. Jackson, "Towards high-power mid-infrared emission from a fiber laser," *Nature Photon.*, vol. 6, no. 7, pp. 423–431, 2012.

[3] M. Krause, D. Steeb, H. J. Foth, J. Weindler, and K. W. Ruprecht, "Ablation of vitreous tissue with erbium: YAG laser," *Invest. Ophtalmol. Vis. Sci.*, vol. 40, no. 6, pp. 1025–1032, 1999.

[4] X. Zhu and N. Peyghambarian, "High-power ZBLAN glass fiber lasers: Review and prospect," *Adv. Optoelectron.*, vol. 2010, pp. 149–154, 2010.

[5] M. Heck *et al.*, "Femtosecond-written long-period gratings in fluoride fibers," *Opt. Lett.*, vol. 43, no. 9, pp. 1994–1997, 2018.

[6] V. Artyushenko *et al.*, "Mid-infrared fiber optics for 1-18 μm range: IR-fibers and waveguides for laser power delivery and spectral sensing," *Optik Photonik*, vol. 9, no. 4, pp. 35–39, 2014.

[7] M. Bernier *et al.*, "Bragg gratings photoinduced in ZBLAN fibers by femtosecond pulses at 800 nm," *Opt. Lett.*, vol. 32, no. 5, pp. 454–456, 2007.

[8] Y. O. Aydin, V. Fortin, R. Vallée, and M. Bernier, "Towards power scaling of 2.8 μm fiber lasers," *Opt. Lett.*, vol. 43, no. 18, pp. 4542–4545, 2018.

[9] E. Ertorer, M. Haque, J. Li, and P. R. Herman, "Femtosecond laser filaments for rapid and flexible writing of fiber Bragg grating," *Opt. Exp.*, vol. 26, no. 7, pp. 9323–9331, 2018.

[10] G. Bharathan, R. I. Woodward, M. Ams, D. D. Hudson, S. D. Jackson, and A. Fuerbach, "Direct inscription of Bragg gratings into coated fluoride fibers for widely tunable and robust mid-infrared lasers," *Opt. Exp.*, vol. 25, no. 24, pp. 30013–30019, 2017.

[11] K. Goya *et al.*, "Plane-by-plane femtosecond laser inscription of first-order fiber Bragg gratings in fluoride glass fiber for *in situ* monitoring of lasing evolution," *Opt. Exp.*, vol. 26, no. 25, pp. 33305–33313, 2018.

[12] G. Bharathan, T. T. Fernandez, M. Ams, R. I. Woodward, D. D. Hudson, and A. Fuerbach, "Optimized laser-written ZBLAN fiber Bragg gratings with high reflectivity and low loss," *Opt. Lett.*, vol. 44, no. 2, pp. 423–426, 2019.

[13] G. Bharathan, T. T. Fernandez, and M. Ams, "Femtosecond laser direct-written fiber Bragg gratings with high reflectivity and low loss at wavelengths beyond 4 μm," *Opt. Lett.*, vol. 45, no. 15, pp. 4316–4319, 2020.

[14] J. Bei *et al.*, "Experimental study of chemical durability of fluorozirconate and fluoroindate glasses in deionized water," *Opt. Mater. Exp.*, vol. 4, no. 6, pp. 1213–1226, 2014.

[15] F. G. Heinz and H. Bruno, "Chemical stability of zrF_4- and AlF_3-based heavy metal fluoride glasses in water," *J. Non-Cryst. Solids*, vol. 284, no. 1, pp. 105–109, 2001.

[16] S. Wang, J. Zhang, N. Xu, S. Jia, G. Brambilla, and P. Wang, "2.9 μm lasing from a Ho^{3+}/Pr^{3+} co-doped AlF_3-based glass fiber pumped by a 1150 nm laser," *Opt. Lett.*, vol. 45, no. 5, pp. 1216–1219, 2020.

[17] M. Liu *et al.*, "Room-temperature watt-level and tunable $\sim$3 μm lasers in ho^{3+}/Pr^{3+} co-doped AlF_3-based glass fiber," *Opt. Lett.*, vol. 46, no. 10, pp. 2417–2420, 2021.

[18] G. D. Marshall, R. J. Williams, N. Jovanovic, M. J. Steel, and M. J. Withford, "Point-by-point written fiber Bragg gratings and their application in complex grating designs," *Opt. Exp.*, vol. 18, no. 19, pp. 19844–19859, 2010.

[19] T. E. Chiamenti, A. Reupert, O. Kara, M. Becker, L. Wondraczek, and M. Chernysheva, "First-order fiber Bragg grating inscription in indium fluoride fiber using a UV/Vis femtosecond laser and two-beam interferometry," *Opt. Lett.*, vol. 46, no. 8, pp. 1816–1819, 2021.

[20] E. Ertorer *et al.*, "Femtosecond laser filaments for rapid and flexible writing of fiber Bragg grating," *Opt. Exp.*, vol. 26, no. 7, pp. 9323–9331, 2018.

[21] X. Sun *et al.*, "Phase-shifted gratings fabricated with femtosecond laser by overlapped two types of fiber Bragg gratings," *Opt. Laser Technol.*, vol. 124, pp. 105969–105974, 2020.